Title

The Continuous Risk Profile Approach for the Identification of High Collision Concentration Locations on Congested Highways

Authors

Chung, Koohong
Ragland, David R.
Madanat, Samer
et al.

Publication Date

2009-07-01

The Continuous Risk Profile Approach for the Identification of High Collision Concentration Locations on Congested Highways

Koohong Chung, California Department of Transportation, David R. Ragland, UC Berkeley Traffic Safety Center, Samer Madanat, Institute of Transportation Studies, UC Berkeley, and Soon Mi Oh, UC Berkeley Traffic Safety Center

UCB-ITS-TSC-2007-6-Updated July 2009

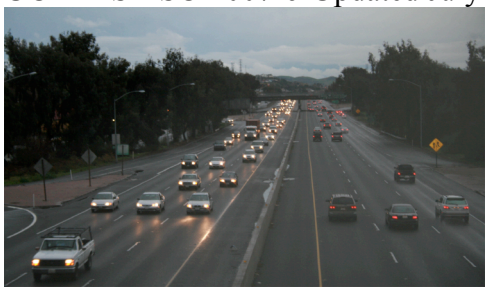

JULY 2009

UNIVERSITY OF CALIFORNIA Berkeley
Traffic Safety Center

THE CONTINUOUS RISK PROFILE APPROACH FOR THE IDENTIFICATION OF HIGH COLLISION CONCENTRATION LOCATIONS ON CONGESTED HIGHWAYS

Koohong Chung, California Department of Transportation, United States; David R. Ragland, University of California, Berkeley, United States; Samer Madanat, University of California, Berkeley, United States; Soon Mi Oh, University of California, Berkeley, United States

Abstract This paper documents a new method for monitoring traffic collision data from continuous roadway facilities to detect high collision concentration locations. Many existing methods for detecting collision concentration locations require segmentation of roadways and assume traffic collision data are spatially uncorrelated, resulting in both false positives (i.e., identifying sites for safety improvements that should not have been selected) and false negatives (i.e., not identifying sites that should have been selected). The proposed method does not require segmentation of roadways; spatial correlation in the collision data does not affect the results of analysis. This new method has a lower false positive rate than the conventional sliding moving window approach. This paper shows how the proposed method can proactively identify high collision concentration locations and capture the benefit of safety improvements observed in the project location and in neighboring sites.

Key words continuous risk profile, traffic collision, proactive approach, effectiveness of countermeasure

1. Introduction

Identifying high collision concentration locations is an important step towards improving the safety of roadways and reducing overall traffic delays resulting from vehicular collisions. Several approaches are currently available for identifying high collision locations (Hauer 1996, Kononov 2002, Hauer et al 2002, California Department of Transportation 2002). For example, the Federal Highway Administration (FHWA) is currently evaluating the suitability of using the concept of Safety Performance Function (SPF) in identifying high collision concentration locations (Federal Highway Administration 2002).

The SPF is used to classify the safety level of service (LOS) for a facility into one of the following ratings: A, B, C or D (Federal Highway Administration

2002), with LOS A being the best. The SPF can be used to detect the sites that have LOS D. However, if the function defining the LOS is not properly estimated, it can result in both false positives (i.e., identifying sites for safety improvements that should not have been selected) and false negatives (i.e., not identifying sites that should have been selected).

In previous research (Kononov and Allery 2002), Safety Performance Functions were estimated using Poisson and Negative Binomial regression on data of similar facilities. This approach is suitable for comparing collision rates of facilities that are isolated in space, such as intersections. However, the approach is not appropriate for continuous facilities such as highway segments because the method implicitly assumes that: (1) the rate of traffic collisions along a highway is spatially uncorrelated; (2) the rate at which collisions occur within the segment remains constant; and (3) the factors causing high collision rates reside within the segment.

In this paper, a new approach for identifying high collision concentration locations is presented. The method, which we call the Continuous Risk Profile (CRP) is not constrained by these three assumptions. Instead, it continuously profiles the true underlying risk, in units of number of collisions per unit distance, along the highway. The presence of spatial correlation in the collision data does not affect the results of the analysis. When the proposed method was applied to 413 miles of roadways in California, it showed a significant improvement in reducing the rate of false positives relative to the method currently used.

In the next section, we describe the problems associated with the estimation of SPF. Then, we describe our proposed CRP approach and present the findings from applying the method to California collision data. The proposed approach can be used to proactively identify high collision concentration locations by monitoring changes in risk over the years and provide a more accurate quantification of the effectiveness of a countermeasure. These applications of the proposed method are discussed prior to ending this paper with a brief summary and discussion of future research.

2. Issues in developing a Safety Performance Function for Freeways

2.1 Are Traffic Collisions in Freeways Independently Distributed?

Fig. 1 is an occupancy contour plot of a 20 mile segment of I-880 Northbound in the San Francisco Bay Area in California shown on a time and space axes; the *x*-axis shows the time and *y*-axis shows distance along the corridor. The traveling direction of the traffic is also indicated in the right side of the figure. The darker re-

gion in Fig. 1(a) indicates congested traffic and the lighter color indicates freely flowing traffic. The 20 mile segment is plagued by three recurrent bottlenecks and these are labeled A, B and C in the figure: bottlenecks A and C activate every week day while B activates less frequently.

Fig. 1(b) shows the same plots with traffic collision data recorded in the Traffic Accident Surveillance and Analysis System (TASAS). The white boxes in the figure denote the time and location of the individual collisions that occurred on the freeway. Six collisions shown in Fig. 1(b) were grouped into two dotted circles labeled I and II, where each dotted circle inscribes three collisions.

The three collisions in circle I all occurred within 35 minutes; they were spaced only 0.1 mile apart. The reported collision times were 18:10, 18:40 and 18:45, but the actual time interval between these collisions may have been even shorter. The first two boxes that are partly overlapping in circle II occurred within 10 minutes of each other and are spaced about 0.1 mile apart. The third collision inscribed in circle II occurred about two mile upstream of where the first two collisions occurred and 15 minutes later in time. In addition to its proximity (in both time and space) to the previous collisions, the third collision occurred where the freely flowing traffic state met with the end of the queue (Fig. 1(b)), where a sudden and pronounced speed reduction in traffic occurs.

The collisions inscribed in circles I and II show how secondary collisions can occur while traffic is congested. The occurrences of the secondary collisions during the congested traffic state were also observed on other days as well as other routes. Fig. 2 shows time-space occupancy contour plots from other days and routes with collisions and incidents (defined as events that can potentially lead to vehicle collisions). The incident data were obtained from the Bay Area Incident Response System.

These figures indicate that traffic collisions are often accompanied by secondary collisions in the vicinity. The upstream collisions are likely to have been caused by sudden and pronounced speed changes due to the downstream collision, while the downstream collisions could have been caused by lane changes drivers make while accelerating as they leave the collision site. These secondary collisions occur due to changes in traffic conditions, and are not necessarily due to deficiencies in the site itself. The observed collision patterns are reproducible phenomena and result in higher collision rates (collisions/distance) in the vicinity of recurrent bottlenecks. Such secondary collisions are one of the possible sources of the spatial correlation observed in traffic collision data. Not accounting for the spatial dependence of traffic collisions in estimating the parameters of the SPF can result in biased estimates.

It should be noted that spatial correlation exists in congested highways but may not be an issue in uncongested highways, such as rural roads.

One remedy for reducing spatial dependence is to increase the size of the highway segments used to estimate the parameters of the SPF. However, this can introduce other problems, which are discussed next.

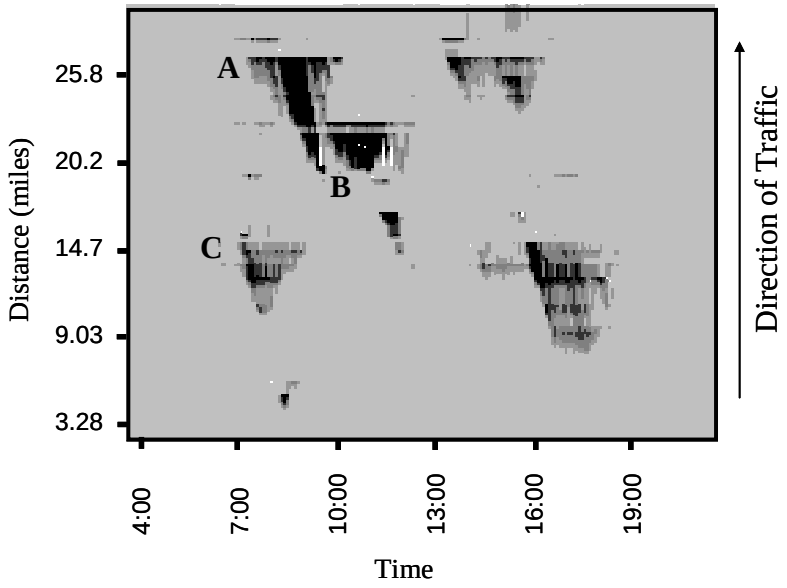

Fig. 1(a). I-880 Northbound, Alameda County, July 9, 2003

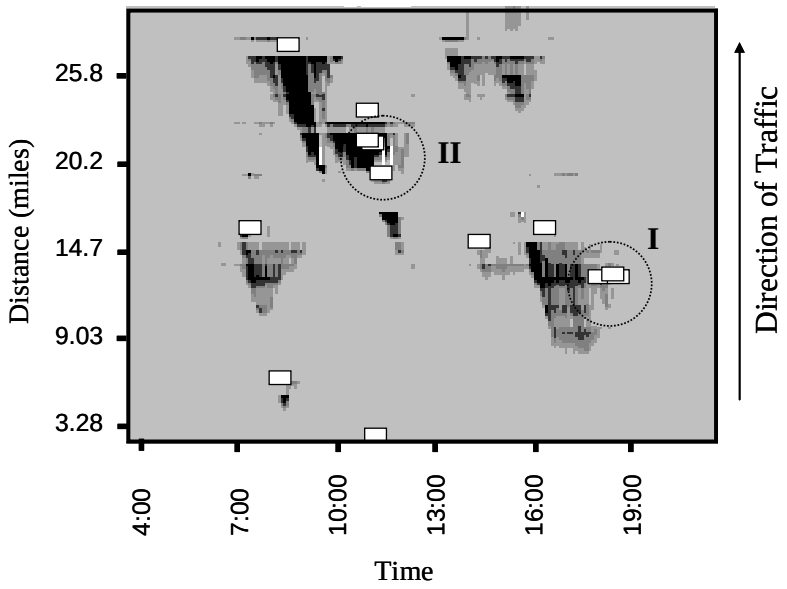

Fig. 1(b). I-880 Northbound, Alameda County, July 9, 2003

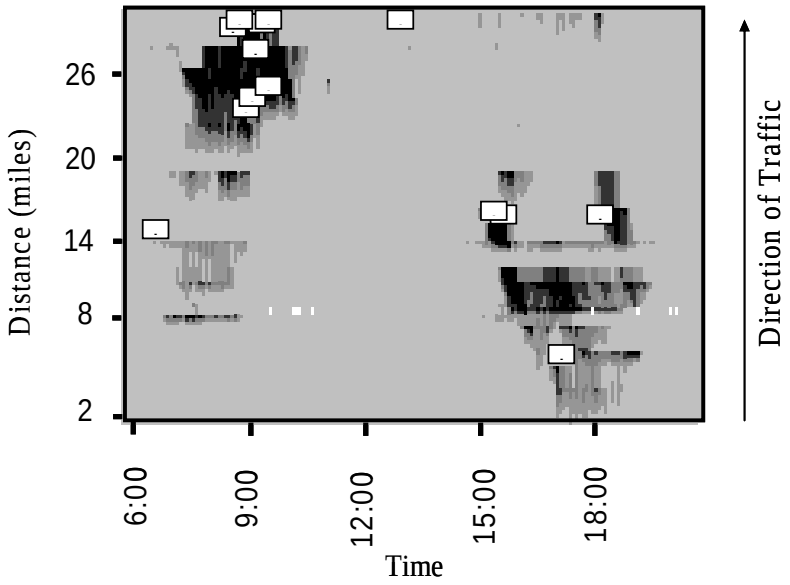

Fig. 2(a). I-880 Northbound, Alameda County, Jan 22, 2004

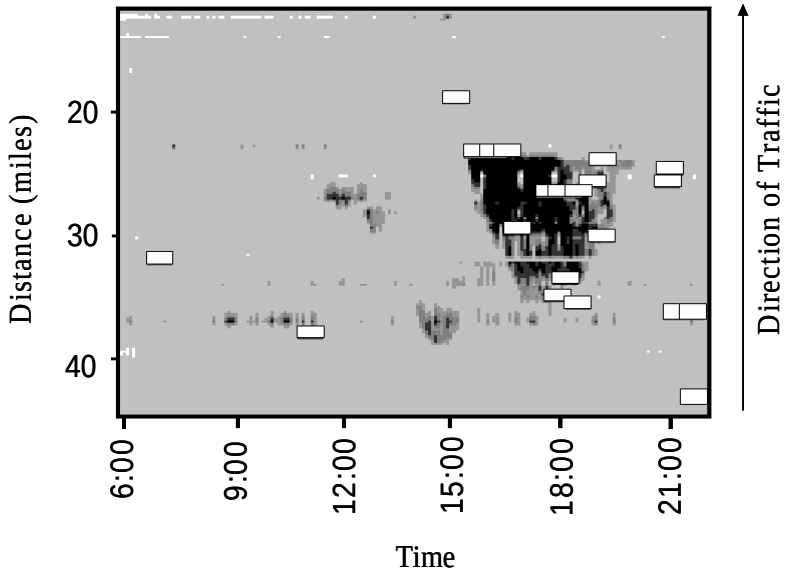

Fig. 2(b). I-880 Southbound, Alameda County, Jun 19, 2004

2.2 Segmentation of Roadways

One remedy for reducing spatial correlation is to increase the size of the segments used to generate data points for estimating SPF. However, if one were to increase the segment length to mitigate spatial correlation, one can extend the segment size to include freeway sections where the geometric features change (i.e., shoulder width, vertical profile and proximity to adjacent ramps). Such changes in geometry need to be incorporated in the estimation process. Failure to reflect the changes in the model will increase the variance of the estimates.

For example, suppose Z_i is an unobserved explanatory variable that affects the collision count μ_i and has a different value in the first and the second half of a segment. X_i is an observed explanatory variable whose value remains constant over the entire segment, and β and π are constants associated with X_i and Z_i. Then, the collision rates for the first and second halves of the segment, μ_1 and μ_2, are:

$$\mu_1 = \exp(\beta X_1 + \pi Z_1) \quad (1)$$

$$\mu_2 = \exp(\beta X_1 + \pi Z_2) \quad (2)$$

However, increasing the segment size without accounting for the change in Z_i restricts the equation to have the following form:

$$\hat{\mu}_1 = \hat{\mu}_2 = \exp(\beta X_1) \quad (3)$$

The observed collision counts are likely to differ from the expected count more than they would if the model were correctly specified (Barron 1992, Pindyck and Rubinfeld 1997). This results in overestimation of the variance and an increase in the false negative rate.

Increasing the segment length can also result in increasing false negatives in another way, since a long segment length can average out highly localized collision rates (Hauer et al. 2002). In this case, high collision concentration locations may not even be detected.

Next, we present a new method for continuously profiling the risk along a roadway that addresses the limitations of approaches that employ highway segmentation.

3. The Continuous Risk Profile Approach

3.1 Method

The CRP shapes itself to the underlying true risk, and produces a measure of risk interpretable as collision density per unit distance of roadway. This method can both proactively and reactively monitor the changes in risk over the years, thus making it also suitable for quantifying the effective of countermeasures. Detailed

discussions of the applications of CRP method are provided later in this paper. A qualitative description of how the CRP is constructed is presented in this section.

The performance of approaches that compare the number of observed collisions with a predetermined number is greatly influenced by the length of the segment used. When it is too long, the approach is not likely to detect localized high collision concentration locations. When it is too short, it can result in high false positive rates (California Department of Transportation 2002).

As a result of analyzing large amounts of empirical data, we have found that the short-lived (in terms of distance) spikes in collisions rates that appear pervasively over a long stretch of roadway are due to statistical fluctuations. Some of these variations can be smoothed by using a moving average as follows (Ljung 1999). This process is further explained with the aid of Figure 3, and equation 4.

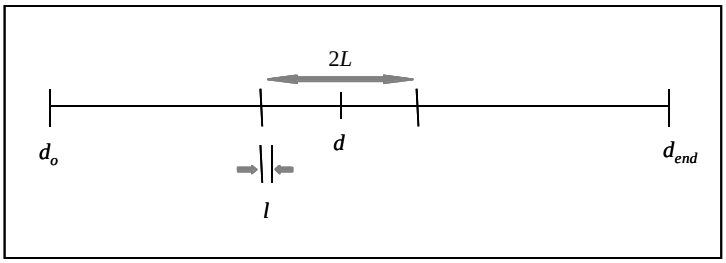

Fig. 3. Hypothetical Highway Segment showing the window used for averaging

Fig. 3 shows a hypothetical highway segment whose starting location is denoted by d_0 and end location by d_{end}. We define the risk at point d as the average collision rate (per unit distance) computed over a window. This window moves from the start of the segment to the end. This averaging of risk over the interval eliminates small fluctuations, but captures gradual changes in risk.

Let $A(d)$ denote the number of collisions per unit distance observed in the vicinity of location d, i.e., within the interval $[d - l/2, d+l/2]$ and $M(d)$ denote the average number of collisions over the window $[d - L, d + L]$. Then, $M(d)$ is given by:

$$M(d) = \frac{\sum_{i=-\min(L/l,(d-d_0)/l)}^{\min(L/l,(d_{end}-d)/l)} A(d + i \times l)}{\min(L/l,(d_{end}-d)/l) + \min(L/l,(d-d_0)/l) + 1} \qquad (4)$$

For

$$d = d_0 + k \times l \quad \text{and} \quad k = 1,2,\ldots \frac{d_{end} - d_0}{l}$$

Where
d_0 = beginning postmile of segment
d_{end} = ending postmile of segment

$d_0 < d_{end}$
l = increment
$2L$ = size of the moving average window
$k, \frac{L}{l}$ and $\frac{d_{end} - d_0}{l}$ are integers (because they define the number of increments within the moving window)

The size of the road segment, $2L$, used to pre-filter the noise determines the appearance of the CRP. There are two considerations in choosing the size of L. One consideration is the amount of data: collision data collected over an extended period of time include less noise and allow the use of a relatively small L. A second consideration is the actual (but not precisely known) variation in risk along a roadway. For example, an extended straight roadway with homogenous feature is likely to have little variation, while a roadway with curves, inclines, or cross streets is likely to have greater variation in risk over small distances. In the former case, a large L is most efficient; in the later case, a smaller L can work more efficiently to capture the variation in risk as long as there is a sufficient period of time for which collision data are available. We have varied $2L$ from 0.01 mile to 1 mile, and determined that 0.2 mile is a suitable choice: a shorter size did not effectively filter out the random fluctuations while a longer size of $2L$ resulted in shifting the locations of peaks in the CRP. We have used 0.2 mile as $2L$ and 0.01 mile as l in the subsequent analysis.

The risk in units of number of collisions per unit distance, in excess of a reference risk, can be plotted by rescaling it by $B(d)$ (see Fig. 4(a)). $B(d)$ can be interpreted as the number of collisions required for significance for the given facility in a unit distance. When the observed collision rate exceeds this value, the site should be reported for safety investigation.

Note that the value of $B(d)$ is constant within the same type of facility but changes discretely when the facility classification changes. The value of $B(d)$ used in Fig. 4(a) is the number of collision required for significance at 99.5% used by the California Department of Transportation (Caltrans) converted to units of number of collisions per unit distance.

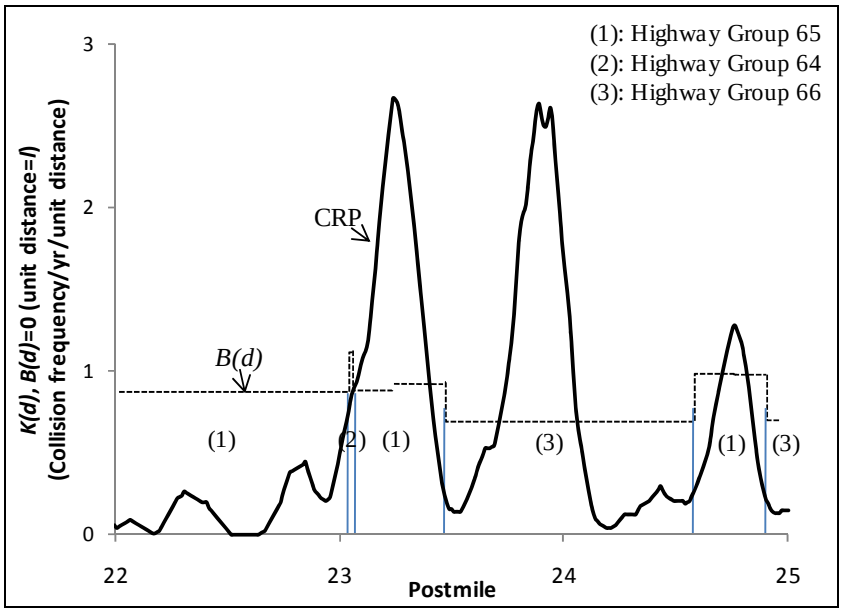

Fig. 4(a). *K(d)* at *B(d)*=0 and *B(d)* at significance at 99.5% , I-880 Northbound 2005

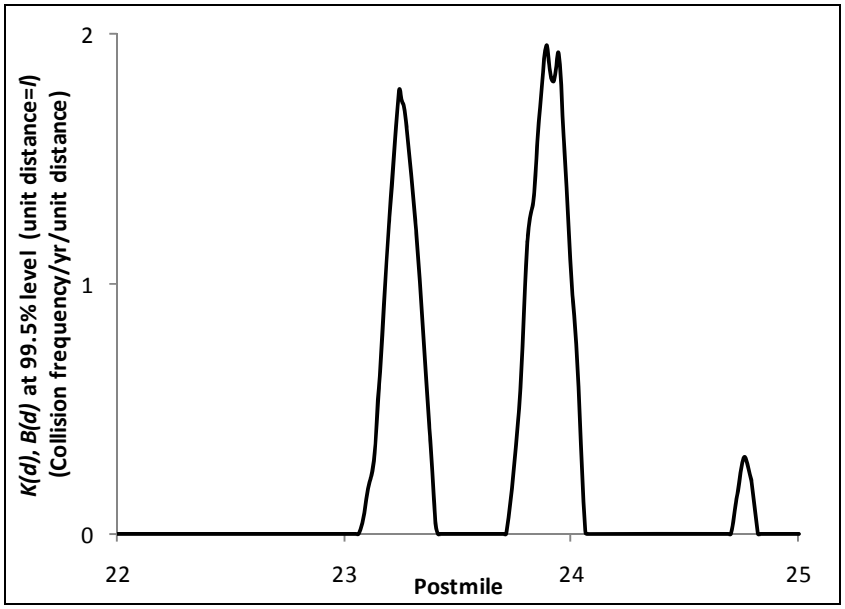

Fig. 4(b). Excess risk at significance of 99.5%, I-880 Northbound 2005

Fig. 4(b) shows the excess collision rate, denoted by *K(d)*. Note that *K(d)* not only identifies high risk locations, but also shows the excess risk in the segment compared to the base risk, *B(d)*. This will allow us to determine where the risk becomes significant as well as locations of the localized peaks. Note that the area under *M(d)* between two locations (spanning greater than 2*L*) is the number of collisions within the segment and the area under *K(d)* is the excess number of collisions.

$$K(d) = Max\left(M(d) - B(d), 0\right) \tag{5}$$

3.2 Comparing the performance of the CRP with that of the Sliding Window Approach

Caltrans monitors traffic collision data in an effort to locate high collision concentration locations using a sliding moving window approach. The approach compares the observed collision rate in a fixed segment length with a pre-determined rate by using equations 6 and 7.

$$N_E = \frac{R_E \times Travel}{10^6} \tag{6}$$

$$N_R = N_E + 2.576(N_E)^{1/2} + 1.329 \tag{7}$$

Where

R_E = Expected collision rate per Vehicle-Mile-Travel (VMT) determined for highway group *E*

N_E = Expected number of collisions for highway group *E*

N_R = Number of collision required to be significant at the 99.5% confidence level

Travel = Average Daily Traffic (ADT) × Number of days × Length

When the observed rate exceeds the pre-determined rate for a given facility type, the site is considered to be a high collision concentration location. If not, the approach slides the window by a small increment and repeats the same analysis.

When potential safety investigation locations are identified, Caltrans safety engineers investigate these locations in detail in order to determine if the site requires some safety improvement. Based on the safety engineers' field report, one can evaluate whether the detected site is a true positive (i.e., identifying sites for safety improvements that should have been selected) or a false positive.

Even when the sites are true positives, investigators do not recommend sites for safety improvement in their report when there is a corridor-wide safety improvement project that is scheduled to include the identified locations. Based on the safety engineers' report and list of corridor wide safety improvement projects, we have identified true positive locations (hotspots). The locations of these true hots-

pots were compared to the sites identified by the proposed and the existing approaches.

Table 1. Performance of the CRP compared to the Sliding Window approach

Route	Length	True Hotspots	Existing Method	CRP
24E	14.0	2	2	2
24W	14.0	3	3	3
580E	76.2	1	2	2
580W	76.3	0	11	4
680N	70.5	0	11	5
680S	70.6	2	4	2
880N	46.0	1	20	1
880S	45.7	0	9	1
Total	413.3	9	62	20
	True positive rate		15%	45%
	False positive rate		85%	55%

The proposed approach was applied to 413 mile of freeways in the San Francisco Bay Area and detected 20 locations that display high collision rates under wet pavement conditions using traffic collision data from 2001 to 2003. These sites were then compared to sites identified under the existing approach. Note that same set of collision data and the same criteria were used: the rate calculated from equation 7 was used as *B(d)* after converting its unit to be consistent with the unit of *M(d)* in constructing the CRP. The results are shown in Table 1. Note that the true hotspots in Table 1 were a subset of the sites identified by the CRP, and those identified by the CRP were a subset of the sites identified by the Caltrans existing method. The locations of the hotspots are known, but are not shown in this paper due to size limitations.

Neither approaches had false negatives: however, the false positive rate of the sliding moving window approach was three times greater. False positives are not as serious as false negatives; the former only means that safety engineers had to examine sites where investigations were not needed. Nevertheless, a high false positive rate leads to suboptimal utilization of resources. In addition to having a lower false positive rate, the CRP approach can also be used to proactively monitor the change in collision rate and estimate the benefit-cost ratio of safety improvement projects. These applications of the CRP are presented next.

4. Other Applications of the CRP

4.1 Proactive Detection of High Collision Concentration Locations

The CRP can proactively monitor the changes in collision rate before the collision rate exceeds the threshold determined by an agency. Fig. 5 shows how the risk varied over a three mile freeway segment during a nine year period. Notice the evolution of the risk profile between the two vertical dotted lines labeled X_1 and X_2. There were no apparent peaks in 1994, but the peak began to emerge in 1997 and continued to grow in the subsequent years.

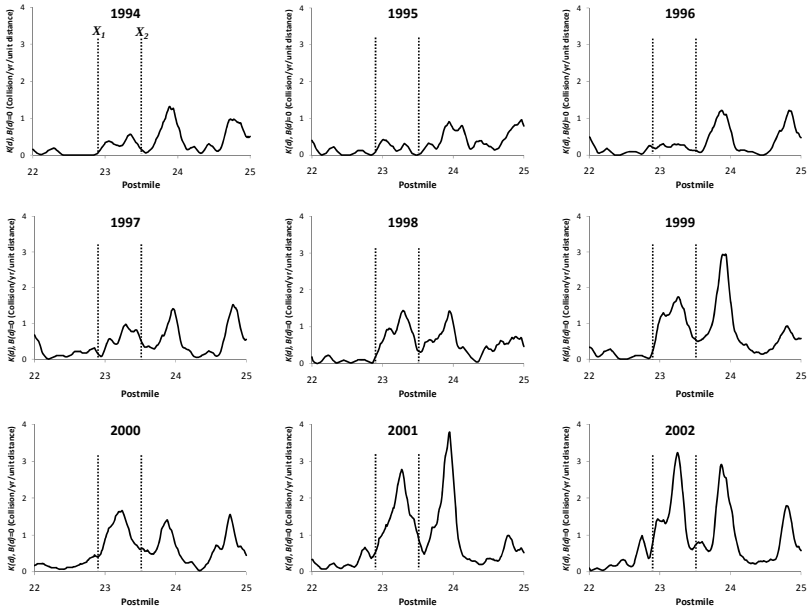

Fig. 5. Evolution of changes in risk (I-880 N, TASAS, 1994~2002) (unit distance=*l*)

Suppose an agency requires safety investigation when the collision rate exceeds *B(d)*. (see Fig. 6(a)). The agency can construct the CRP with *B'(d)* where *B'(d)* < *B(d)* (see Fig. 6(b)). In both figures, the *x*-axis in the figure is the postmile and the *y*-axis shows the excess collision rate, *K(d)*. The area under the curve indicates the excess number of collisions.

Notice how the peak labeled *A'* only appears in 6(b) and not in 6(a) in 2000. By using *B'(d)*, the agency can locate the peaks that are not yet significant at the *B(d)*

level. The location of the peak, *P*, can be determined within the stretch of roadway between X_1 and X_2 (see Fig. 6(b)) before the CRP exceeds the threshold level. This is possible because the locations of the peaks are highly reproducible in the CRP from year to year, even though the scales of the peaks are not.

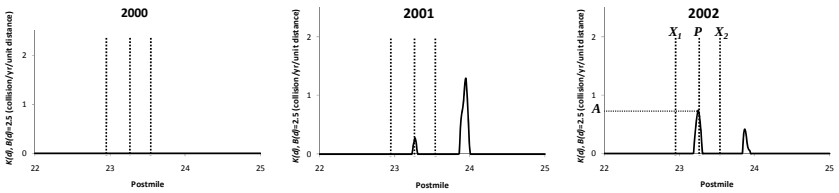

(a) *B(d)* = 2.5 collision/yr/unit distance

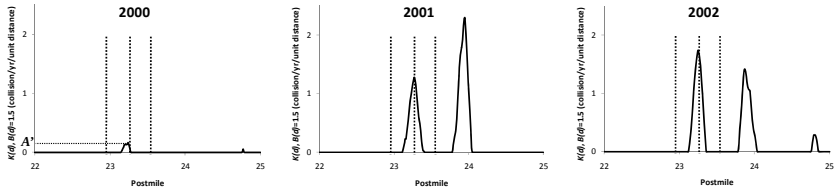

(b) *B'(d)* = 1.5 collision/yr/unit distance

Fig. 6. Detection of changes in risk (I-880 N, TASAS, 2000~2002) (unit distance=*l*)

To demonstrate this, we normalized the magnitudes of the peaks such that the area under the curve between X_1 and X_2 is 1. The magnitude of the CRP peak between X_1 and X_2 is normalized by using the following equation:

$$S(d) = \frac{K(d)}{\int_{X_1}^{X_2} K(d)dx} \tag{8}$$

where
X_1 = starting post mile of interest area
X_2 = end post mile of interest area

This is shown in Figure 7.

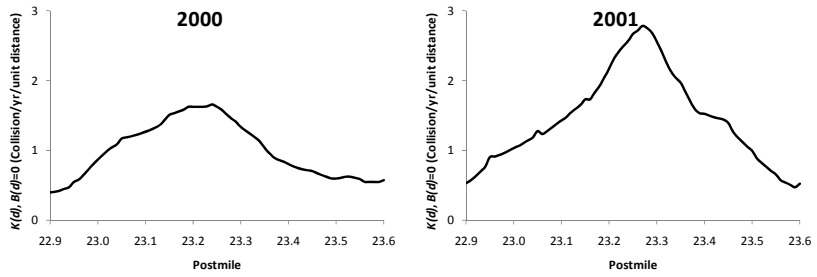

(a) CRP

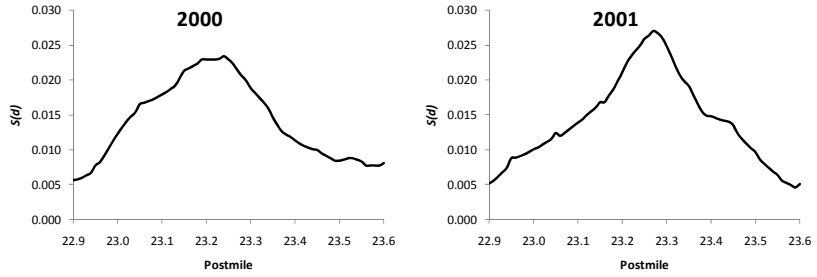

(b) Normalized CRP

Fig. 7. Normalizing the CRP from 2000 by 2001 (unit distance=*l*)

To test the reproducibility of the peak locations over time, we computed the cross-correlation of the normalized CRP magnitudes for a range of locations around the normalized peaks by using equation (9):

$$r_{y,y-1}(i) = \frac{\sum_d (S_y(d) - \bar{S}_y)(S_{y-1}(d-i) - \bar{S}_{y-1})}{\sqrt{\sum_d (S_y(d) - \bar{S}_y)^2}\sqrt{\sum_d (S_{y-1}(d-i) - \bar{S}_{y-1})^2}} \quad (9)$$

where

$r_{y,y-1}(i)$ = cross-correlation between two successive values of *K(d)*, in years *y* and *y*-1, obtained by shifting *K(d)* in year *y*-1 by a distance *i*

$S_y(d) = S(d)$ in year *y*

$\bar{S}_y$ & $\bar{S}_{y-1}$ = means of the corresponding series

$-0.5 < i < 0.5$, where *i* was incremented by 0.01 miles

Equation (9) was used to compute the cross-correlations of the normalized risks between year 2000 and other years from 1997 to 2002. For each pair, the cross-

correlation was calculated for a range of locations of the other year's cluster. The cluster was shifted from its original location in a range of distances, from -0.5 to 0.5 miles by increments of 0.01 miles from its original location. Fig. 8 shows the result of the cross-year correlations (Chung et al 2006, Mauch and Cassidy 2002). The x-axis represents the distance shifted (in 0.01 mile increments) and the y-axis the correlation resulting from shifting the curves. For most cases, the correlation is greatest when the curve is not shifted; it drops quickly with relatively small shifts. These findings show that the locations of the peak are highly reproducible, although the magnitude of the excess number of collisions grew over the years.

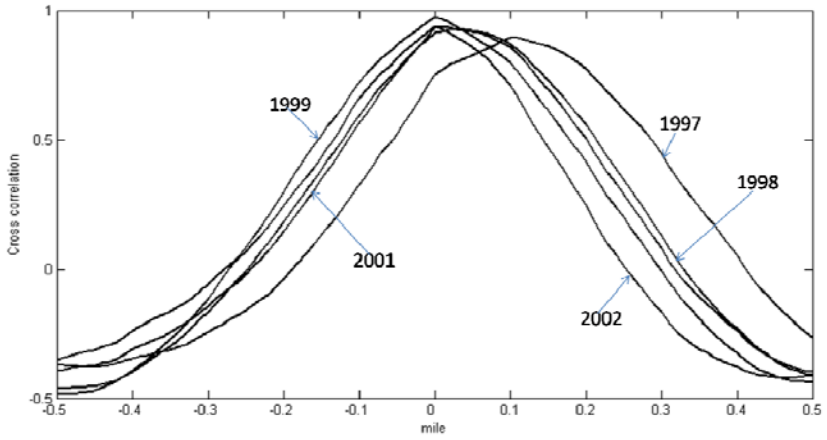

Fig. 8. Cross correlations between the CRP values in 2000 and other years in the neighborhood of the peak

Table 2. Cross correlation between 2000 and other years

Year	Shift (miles)	Maximum cross correlation coefficient
1997	0.10	0.90
1998	0.03	0.93
1999	0.00	0.97
2001	0.00	0.93
2002	0.00	0.94

Table 2 shows the highest correlation and its corresponding shift for each comparison. Notice the high correlation and the reproducibility of the peak locations, indicated by a maximum correlation obtained by a small or no shift of $S(d)$ in 2000: the small variation could have been the result of how the data were collected in early years or variations in reported collision locations.

Fig. 9 shows the ratio of the areas under $S(d)$ within X_1 and X_2 in 2000 and in other years. The area under the CRP between X_1 and X_2 remains low until 1997

and then increases linearly until 2002 as indicated by the dotted line. Using *B(d)*, the criterion set by an agency, the location P would not have been detected in 2000. However, using *B'(d)* and making use of the reproducibility of the peak patterns, the agency can proactively detect critical sites in cases when the collision rate increases progressively.

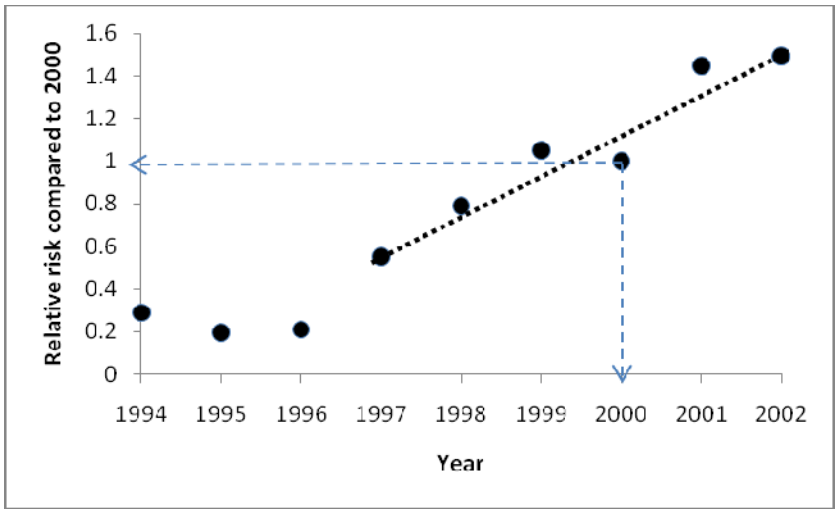

Fig. 9. Relative risk compared to 2000

4.2 Quantifying the benefit-cost ratio of a countermeasure

The traffic collision data plotted on top of the time-space contour plot (Fig. 2) showed how a vehicle collision can cause secondary collisions not only in the vicinity but also a few miles upstream. Since traffic collisions are not spatially independent, an improvement made on a roadway may not only enhance the safety level of the facility within the project site but also in neighboring locations. Fig. 10 shows an example of such a case.

The figure shows how the risk varied over five year period along a 5-mile of freeway segment in I-55 Northbound in Orange County, California. A countermeasure was implemented on this freeway, between postmiles 13.8 and 15.2 in 2001; Fig. 10 shows that the peaks that resided within the project scope prior to 2001 disappeared after the project was implemented in 2001. Notably, other peaks between X_S and X_E located outside of the project scope also disappeared. Using the CRP method, one can capture the spillover benefit, by comparing the risk profile in the vicinity of the project site before and after the improvement, and thus avoid underestimating the project's benefit.

The number of collisions observed within the project scope and segment between location S_1 and S_2 are shown in Table 3. Even a simple comparison of collision frequencies before and after the construction reveals that only accounting for the changes in collision frequency underestimates the benefit of the project. In the example shown in Fig. 10, a net reduction of 32 collisions was observed during the two year period after the construction compared to the two year period prior to the construction, while a reduction of 180 collisions was observed between X_S and X_E. Using the average collision cost in California, the estimated monetary savings to the public estimated is 1,293,000 dollars for the roadway length within the project scope, and 7,272,000 dollars for the entire extent of the roadway.

Therefore, the benefit-cost ratio calculated by accounting only for collision reductions within the project scope may underestimate the effectiveness of the countermeasure (Hauer 1997).

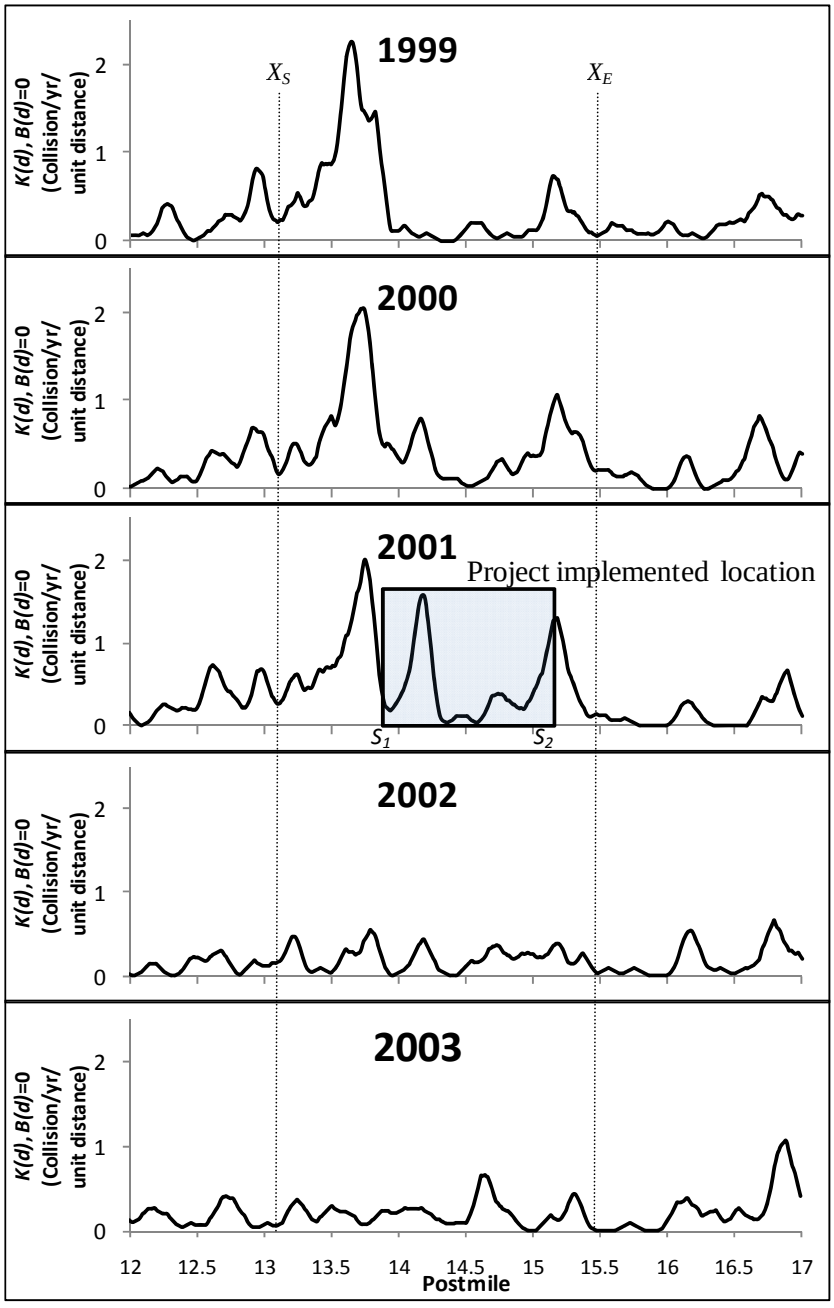

Fig. 10. Change of CRP before and after improvement (I-55 N, TASAS, 1999~2003)

Table 3. Comparison of before & after improvement

	Project limits	CRP limits
Number of collisions before improvement (1999~2000)	124	329
Number of collisions after improvement (2002~2003)	92	149
Net change	32	180
Benefit (in 1000s of dollars)	1293	7272

5. Conclusion

Current approaches for identifying high collision concentration locations require segmentation of roadways for the purpose of estimating the parameters of safety performance functions (SPF). These approaches assume that: (1) the rate of traffic collisions along a highway is spatially uncorrelated; (2) the rate at which collisions occur within the segment remains constant; and (3) the factors causing high collision rates reside within the segment.

Assumption (1) is found to be not true for traffic collisions that occur on congested freeways; thus, these approaches can result in erroneous estimates. One remedy for mitigating spatial correlation is to increase the segment size: however, this can lead to violating assumption (2), which leads to an increase in the variance of the estimate, and thus an increase in the false negative rate. Violation of assumption (3) increases the false positive rate, which causes suboptimal utilization of resources.

The continuous risk profile, a new approach for identifying high collision concentration locations, has been presented in this paper. This approach is not constrained by these three assumptions. Instead, it continuously profiles the true underlying risk, in units of number of collisions per mile. The CRP approach was used to detect high collision concentration locations along 413 miles of roadways in California and found to have a lower false positive rate than a conventional sliding window approach. The CRP approach can also be applied to detect critical sites in cases when the collision rate increases progressively over time. This paper also demonstrated how the CRP approach can quantify the spillover benefit of a countermeasure.

Acknowledgments The authors would like to thank the following engineers at the California Department of Transportation (Caltrans) for their help and valuable comments: Larry Orcutt in the Division of Research and Innovation; Sean Nozzari, David Seriani, Rodney Oto, Roland Au-Yeung, Emily Tang, and Kapsoon Capulong in Caltrans District 4 for their time and valuable comments. The authors also benefited from the comments of three anonymous reviewers.

References

Barron, D.N. (1992). The Analysis of Count Data: Overdispersion and Autocorrelation , *Sociological Methodology*, Vol. 22, pp. 179-220

Hauer, E. (1996). Identification of Sites with Promise. *Transportation Research Record*, No. 1542, pp. 54-60.

Hauer, E. (1997). *Observational before-after studies in road safety*. Pergamon, Elsevier Science Ltd.

Ljung, L. (1999). *System Identification –Theory for the User*. Prentice-Hall, Upper Saddle River, New Jersey.

Kononov, J. (2002). Identifying Location with Potential for Accident Reductions: Use of Direct Diagnostics and Pattern Recognition Methodologies. *Transportation Research Record*, No. 1784, pp. 153-158.

Pindyck, R.S., and D.L. Rubinfeld. (1997). *Econometric Models and Economic Forecasts book*. 4th edition, McGraw-Hill/Irwin.

Mauch, M., and M. J. Cassidy. (2002). Freeway Traffic Oscillations: Observations and Predictions. *International Symposium of Traffic and Transportation Theory*, (M. A. P. Taylor, Ed) Pergamon, New York, pp. 653-674.

Kononov, J., and B. Allery. (2003). Level of Service of Safety. In *Transportation Research Record: Journal of the Transportation Research Board*, No. 1840, TRB, National Research Council, Washington, D.C., pp. 57-66.

Hauer, E., J. Kononov, B. Allery, and M. Griffith. (2002). Screening the Road Network for Sites with Promise. *Transportation Research Record*, No. 1784, pp. 27-32.

California Department of Transportation. (2002). *Table C Task Force: Summary Report of Task Force's Findings and Recommendations.* Caltrans.

Federal Highway Administration. (2002). Safety Analyst: Software Tools for Safety Management of Specific Highway Sites. White paper.

Chung, K., J. Rudjanakanoknad, and M. J. Cassidy. (2006).Relation between Traffic Density and Capacity Drop at Three Freeway Bottlenecks. *Transportation Research B*, Vol. 41, Issue 1, pp. 82-95.